NeuroImage: Clinical 38 (2023) 103416

Contents lists available at ScienceDirect

NeuroImage: Clinical

journal homepage: www.elsevier.com/locate/ynicl

The heterogeneity of asymmetric tau distribution is associated with an early age at onset and poor prognosis in Alzheimer's disease

Jiaying Lu [a,b,1], Zhengwei Zhang [a,1], Ping Wu [a], Xiaoniu Liang [c], Huiwei Zhang [a], Jimin Hong [b], Christoph Clement [b], Tzu-Chen Yen [d], Saineng Ding [c], Min Wang [e,f], Zhenxu Xiao [c], Axel Rominger [b], Kuangyu Shi [b,f], Yihui Guan [a,g,h,2,*], Chuantao Zuo [a,g,h,2,*], Qianhua Zhao [c,g,h,i,2,*], for the Alzheimer's Disease Neuroimaging Initiative, for the Shanghai Memory Study

[a] Department of Nuclear Medicine & PET Center, Huashan Hospital, Fudan University, Shanghai, China
[b] Department of Nuclear Medicine, Inselspital Bern, University Hospital, University of Bern, Bern, Switzerland
[c] Department of Neurology, Huashan Hospital, Fudan University, Shanghai, China
[d] APRINOIA Therapeutics Co., Ltd, Suzhou, China
[e] Shanghai Institute for Advanced Communication and Data Science, Shanghai University, Shanghai, China
[f] Department of Informatics, Technische Universität München, Munich, Germany
[g] National Clinical Research Center for Aging and Medicine, Huashan Hospital, Fudan University, Shanghai, China
[h] National Center for Neurological Disorders, Huashan Hospital, Fudan University, Shanghai, China
[i] MOE Frontiers Center for Brain Science, Fudan University, Shanghai, China

ARTICLE INFO

Keywords:
Asymmetry
Tau
Positron emission tomography
Alzheimer's disease
Age
Prognosis

ABSTRACT

Purpose: Left-right asymmetry, an important feature of brain development, has been implicated in neurodegenerative diseases, although it's less discussed in typical Alzheimer's disease (AD). We sought to investigate whether asymmetric tau deposition plays a potential role in AD heterogeneity.

Methods: Two independent cohorts consisting of patients with mild cognitive impairment due to AD and AD dementia with tau PET imaging were enrolled [the Alzheimer's Disease Neuroimaging Initiative (ADNI) cohort with ^{18}F-Flortaucipir, the Shanghai Memory Study (SMS) cohort with ^{18}F-Florzolotau]. Based on the absolute global tau interhemispheric differences, each cohort was divided into two groups (asymmetric *versus* symmetric tau distribution). The two groups were cross-sectionally compared in terms of demographic, cognitive characteristics, and pathological burden. The cognitive decline trajectories were analyzed longitudinally.

Results: Fourteen (23.3%) and 42 (48.3%) patients in the ADNI and SMS cohorts showed an asymmetric tau distribution, respectively. An asymmetric tau distribution was associated with an earlier age at disease onset (proportion of early-onset AD: ADNI/SMS/combined cohorts, $p = 0.093/0.026/0.001$) and more severe pathological burden (*i.e.*, global tau burden: ADNI/SMS cohorts, $p < 0.001/= 0.007$). And patients with an asymmetric tau distribution were characterized by a steeper cognitive decline longitudinally (*i.e.*, the annual decline of Mini-Mental Status Examination score: ADNI/SMS/combined cohorts, $p = 0.053$ / 0.035 / < 0.001).

Conclusions: Asymmetry in tau deposition, which may be associated with an earlier age at onset, more severe pathological burden, and a steeper cognitive decline, is potentially an important characteristic of AD heterogeneity.

* Corresponding authors at: Department of Nuclear Medicine & PET Center, Huashan Hospital, Fudan University, 518 East Wuzhong Road, Shanghai 200235, China (C. Zuo, Y. Guan); Department of Neurology, Huashan Hospital, Fudan University, 12 Middle Wulumuqi Road, Shanghai 200040, China (Q. Zhao).
E-mail addresses: guanyihui@hotmail.com (Y. Guan), zuochuantao@fudan.edu.cn (C. Zuo), qianhuazhao@fudan.edu.cn (Q. Zhao).
[1] These authors contributed equally to this work.
[2] These authors jointly supervised this work.

https://doi.org/10.1016/j.nicl.2023.103416
Received 13 February 2023; Received in revised form 13 April 2023; Accepted 22 April 2023
Available online 28 April 2023

1. Introduction

The bilateral brain hemispheres are characterized by anatomical and molecular left–right asymmetry, which plays an important role in their functional specialization (Duboc et al., 2015). The presence of an asymmetric brain involvement has been reported for several neurological disorders – including Parkinson's disease (PD) (Samii et al., 2004), frontotemporal lobar degeneration (FTLD) (Bang et al., 2015), and corticobasal degeneration (CBD) (Di Stasio et al., 2019). While *post-mortem* pathology studies are generally conducted on a single brain hemisphere, *in vivo* positron emission tomography (PET) imaging offers a valuable opportunity to investigate the presence of an asymmetric pattern of brain involvement under different disease conditions and to examine its clinical implications.

As the most common neurodegenerative disease, the etiology and clinical heterogeneity of Alzheimer's disease (AD) are increasingly recognized as important features that require more attention (Knopman et al., 2021). Brain PET imaging, especially amyloid and tau PET imaging, plays an important role in decoding etiological heterogeneity due to its ability to capture spatiotemporal trajectories of pathological burden *in vivo* (Chhatwal et al., 2022; Collij et al., 2022; Vogel et al., 2021). With the development of PET imaging technology, to visualize the core etiology of AD in the living brains is possible. Thus, a growing number of studies (Frings et al., 2015; Vogel et al., 2021; Yoon et al., 2021; Young et al., 2022) have reported the potential role of asymmetric pathological distribution in AD heterogeneity, including but not limited to atypical AD within the biological "A/T/N" ("A": β-amyloid; "T": tau; "N": neurodegeneration or neuronal injury) scheme (Jack et al., 2018). Among them, the role of asymmetrical tau pattern in AD heterogeneity is relatively less discussed. Two studies recently reported the non-negligible asymmetric tau distribution in the population from normal cognition to AD dementia based on tau PET imaging (Vogel et al., 2021; Young et al., 2022). Work by Vogel and colleagues identified asymmetric tau involvement as one of the hallmarks of the lateral temporal subtype, but no further in-depth exploration was conducted as it was off topic (Vogel et al., 2021). Young et al., focused on the disproportionate cortical tau signal relative to medial temporal lobe in preclinical AD (Young et al., 2022), the asymmetric tau accumulation in other regions as well as the symptomatic phase of AD remains to be explored. Given that the tau molecular diversity is believed as a proxy for the clinical variability of AD (Dujardin et al., 2020) and the amount as well as anatomical localization of tau aggregates (neurofibrillary tangles) across the cerebral cortex parallels clinical phenotype (Ossenkoppele et al., 2016) and disease severity (Arriagada et al., 1992), it's necessary to further explore the potential clinical, pathologic, and prognostic implications of an asymmetric tau burden, which holds promise to improve our pathophysiological understanding, optimize clinical management, and open novel therapeutic paths.

2. Methods

2.1. Participants

Two ethnically distinct independent cohorts were enrolled. One was drawn from the Alzheimer's Disease Neuroimaging Initiative (ADNI)3, in which all participants were Caucasian and underwent tau PET imaging using the first-generation tau tracer ^{18}F-Flortaucipir (also termed ^{18}F-AV-1451) (Marquié et al., 2015). The other was derived from the Shanghai Memory Study (SMS), in which all subjects were Asian and underwent PET tau imaging with the second-generation tau tracer ^{18}F-Florzolotau (also termed ^{18}F-PM-PBB3, or ^{18}F-APN-1607) (Tagai et al., 2021). The SMS was a hospital-based cohort investigation carried out in the memory clinic of the Department of Neurology, Huashan Hospital (Shanghai, China).

Subjects underwent tau PET imaging, structural magnetic resonance imaging (MRI), and neuropsychological test within six months were screened for inclusion. The inclusion criteria for patients with AD of both cohorts included the following: (1) clinical diagnosis of either mild cognitive impairment (MCI) or AD (Albert et al., 2011; McKhann et al., 2011); (2) confirmed positive amyloid PET scan (A +) (^{18}F-Florbetapir: global standardized uptake value ratio (SUVR) $>$ 1.11 (Landau and Jagust, 2015); or ^{11}C-PIB: visual assessment by two independent experienced neuroradiologists (Lundeen et al., 2018)). The details for defining positive amyloid PET scan are showed in Supplementary Methods. Healthy controls (HCs) were also included for the purpose of tau SUVR Z-transformation. The inclusion criteria for HCs in the ADNI cohort included the following: (1) clinical diagnosis of unimpaired cognition; (2) confirmed negative amyloid PET scan (A-); (3) performed normal on cognitive screening [Mini-Mental Status Examination (MMSE) $\geq$ 26]. The inclusion criteria for HCs in the SMS cohort included the following: (1) no complaints of impairment in terms of cognition and instrumental activities of daily living; (2) no history of neurological and psychiatric disorders; (3) performed normal on cognitive screening (MMSE $\geq$ 26). The following exclusion criteria were applied to all participants: (1) showed significant structural brain abnormalities (*i.e.*, brain tumor; traumatic brain injury); (2) poor image quality and/or co-registration in imaging processing (*i.e.,* movement artifacts). Besides, in the SMS cohort, patients with atypical AD were also excluded (Dubois et al., 2014), because asymmetric pathological burden is traditionally thought to be commonly existed in atypical AD (Gefen et al., 2012; Lehmann et al., 2013; Nasrallah et al., 2018; Ohm et al., 2020; Tetzloff et al., 2018), and the admixture of atypical AD may reduce the level of evidence. Furthermore, such exclusion was not performed in the ADNI cohort as no clinical subtype information was provided. All procedures involving human subjects complied with the ethical standards set forth by the Institutional Review Boards of ADNI and the Huashan Hospital (Shanghai, China; No. 2018–363 and 2019–551). Written informed consent was obtained from all participants and/or their legal proxy.

2.2. Demographics and clinical assessment

Age at baseline, age at onset, sex, education (years), and apolipoprotein E (APOE) genotype were collected. APOE ε4-positivity was defined as the presence of at least one APOE ε4 allele. When used as a covariate, the APOE ε4 status was defined as the number of APOE ε4 alleles (0, 1, or 2). Scores on neuropsychological tests of global cognition, instrumental activities of daily living, memory, and executive functions were collected in the ADNI cohort. As for the SMS cohort, an extensive battery of neuropsychological tests that included global cognition, instrumental activities of daily living, memory, visuospatial, language, attention, and executive functions was conducted. The details are summarized in the **Supplementary Methods.** On analyzing patients who had follow-up data, an annual decrease of MMSE scores $\geq$ 6 was considered as a rapid cognitive decline (RCD) (Schmidt et al., 2011; Soto et al., 2008). All other patients were regarded as having a normal cognitive decline (NCD).

2.3. Quantification of plasma biomarkers

In the SMS cohort, all patients underwent measurements of plasma amyloid [amyloid beta(Aβ)40, Aβ42], tau [phosphorylated tau at threonine181 (P-tau181)], and neurodegeneration [total-tau (T-tau), neurofilament protein light chain (NfL)] biomarkers using Quanterix' Single molecule array (Simoa) ® HD-X technology. Notably, plasma Aβ42 to Aβ40 (Aβ42/Aβ40) ratio and P-tau181 to Aβ42 (P-tau 181/Aβ42) ratio were further calculated served as the indices for assessing the amyloid and tau burdens (Chong et al., 2021). The procedures used for sample collection and laboratory analysis have been previously described in detail (Xiao et al., 2021).

2.4. Imaging acquisition and processing

The imaging acquisition protocols for the ADNI cohort can be accessed at http://adni.loni.usc.edu/methods/mri-tool/mri-acquisition/ and http://adni.loni.usc.edu/methods/pet-analysis-method/pet-analysis/. The acquisition protocols for the SMS cohort have been previously reported (Li et al., 2021; Shi et al., 2020).

The raw structural MRI and tau PET data were processed according to the following steps (Li et al., 2021): (1) co-registered the tau PET imaging to the corresponding structural MRI; (2) spatially normalized the tau PET imaging into the Montreal Neurological Institute standard space with the transformation matrices of segmented individual structural MRI, and then smoothed (full-width at half-maximum: 6 mm); (3) performed intensity normalization using cerebellar gray matter as a reference region. All procedures were undertaken using Statistical Parametric Mapping 12 (https://www.fil.ion.ucl.ac.uk/spm/software/spm12/) implemented in MATLAB (MathWorks, Natick, MA, USA).

2.5. Definition of asymmetric versus symmetric tau distribution

Mean global tau SUVR values of each hemisphere were extracted from the combined cortical regions of interest using the Automated Anatomical Labelling Atlas 3 template (Rolls et al., 2020). The regions used for global SUVR quantification are listed in **Supplementary** Table 1. Bilateral tau SUVR values of each patient were then Z-transformed separately in each cohort using the following formula: Z-score = (crude SUVR measured in each patient - mean SUVR measured in HCs) / standard deviation of SUVR in HCs. An absolute global asymmetry score (*abs*GAS) – which was defined as the absolute difference between the Z-score of the bilateral hemispheres was subsequently assigned. Patients with an *abs*GAS ≥ 1 were considered as having an asymmetric tau distribution, whereas an *abs*GAS < 1 denoted a symmetric tau pattern (Buciuc et al., 2021; Tetzloff et al., 2018). The asymmetric group were further divided into the left- and right-predominant subgroups according to the side showing the most severe tau burden.

2.6. Statistical analysis

Statistical analyses were conducted in either cohort separately or grouped together, as appropriate. The asymmetric and symmetric groups were compared on baseline characteristics using the chi-square test, the Student's *t*-test, or the Mann-Whitney *U* test, as appropriate. The intergroup differences in terms of baseline cognitive performance were compared with the generalized linear model (GLM) after adjustment for age and disease duration at baseline, education (years), APOE ε4 status, and sex. The difference in terms of RCD proportion was also investigated by GLM using the baseline MMSE score as an additional covariate. To analyze the longitudinal changes in cognitive decline, the linear mixed-effect model (LMEM) was applied after adjustment for age at baseline, education (years), APOE ε4 status, and sex. Disease duration was used as a time scale. A participant-specific random effect was implemented because of the intraindividual correlations for repeated measurements. To rule out the potential confounding effect of age at onset, the subgroup of EOAD (early-onset AD, defined as a disease onset at<65 years of age) or late-onset AD (LOAD) was further adjusted in the LMEM. When combining two cohorts, different cohort was also considered as a covariate. All analyses were undertaken in SPSS22 (IBM, Armonk, NY, USA), the only exception being the LMEM – which was run in the R environment (Vienna, Austria, https://www.R-project.org/). Two-tailed p values < 0.05 were considered statistically significant.

3. Results

The sample consisted of 217 subjects (Table 1 and Supplementary Table 2). Sixty cognitively impaired participants within the Alzheimer's continuum (A +) and 40 HCs (A-) were from ADNI, whereas 87 cognitively impaired participants within the Alzheimer's continuum (A +) and 30 HCs were from SMS. In the ADNI cohort, there were no significant differences in age and sex between the patient group and the HC group, but the former had shorter years of education ($p = 0.049$), more APOE ε4 carriers ($p < 0.001$), and worse cognitive function ($p < 0.001$) than the latter. In the SMS cohort, no sex difference was found, while the patient group was older ($p < 0.001$), less educated ($p = 0.020$) and worse in cognitive function ($p < 0.001$) than the HC group.

Table 1
Demographic and clinical characteristics of subjects in the two cohorts.

	ADNI (^{18}F-Flortaucipir) cohort (n = 100)		*SMS (^{18}F-Florzolotau) cohort (n = 117)*	
	MCI/AD (n = 60)	*HCs (n = 40)*	*MCI/AD (n = 87)*	*HCs (n = 30)*
Age at baseline (years)	*77.6 ± 8.3*	*75.1 ± 7.1*	*66.2 ± 9.7*	*58.5 ± 8.2*
Female/ Male (Female, %)	*24/36 (40.0%)*	*23/17 (57.5%)*	*58/29 (66.7%)*	*17/13 (56.7%)*
Education (years)	*15.5 ± 2.4*	*16.5 ± 2.7*	*10.3 ± 3.8*	*12.2 ± 3.7*
APOE ε4 -positive/ negative (positive, %) [1]	*35/24 (59.3%)*	*8/32 (20.0%)*	*56/30 (65.1%)*	*N.A.*
MCI/AD (MCI, %)	*41/19 (68.3%)*	*/*	*33/54 (37.9%)*	*/*
Age at onset (years)	*70.2 ± 7.6*	*/*	*63.9 ± 10.1*	*/*
EOAD/LOAD (EOAD, %)	*12/48 (20.0%)*	*/*	*41/46 (47.1%)*	*/*
Disease duration (years)	*7.5 ± 4.6*	*/*	*2.2 ± 1.9*	*/*
MMSE	*23.3 ± 4.9*	*29.0 ± 1.1*	*20.4 ± 6.5*	*28.2 ± 1.4*
MOCA	*18.0 ± 5.7*	*26.9 ± 2.1*	*14.1 ± 6.0*	*N.A.*
CDRSB	*4.6 ± 3.6*	*0.1 ± 0.3*	*6.9 ± 3.4*	*N.A.*
FAQ	*12.0 ± 9.2*	*0.2 ± 0.6*	*14.3 ± 6.9*	*N.A.*

Data are presented as mean ± standard deviation unless otherwise specified.
Abbreviations: ADNI, Alzheimer's Disease Neuroimaging Initiative; SMS, Shanghai Memory Study; APOE, Apolipoprotein E; MCI, mild cognitive impairment; AD, Alzheimer's disease; HCs: cognitively healthy controls; EOAD, early-onset AD; LOAD, late-onset AD; MMSE, Mini-Mental Status Examination; MOCA, Montreal Cognitive Assessment; CDRSB, Clinical Dementia Rating, Sum of Boxes; FAQ, Functional Assessment Questionnaire; N.A., not available.
[1] The presence of at least one APOE ε4 allele was regarded as APOE ε4-positivity. Data on the APOE genotype from the ADNI cohort and from the SMS cohort were missing for one patient, respectively.

The longitudinal cohort with complete follow-up data consisted of 39 (65.0%) and 52 patients (59.8%) from ADNI and SMS, respectively. Fifteen patients from ADNI (maximum follow-up duration: 4 years) and 12 from SMS (maximum follow-up duration: 3.5 years) had undergone at least two follow-up visits after tau PET.

A total of 14 (23.3%) and 42 (48.3%) patients from ADNI and SMS, respectively, had asymmetric tau distribution. The median (interquartile range) *abs*GAS scores in the asymmetric *versus* symmetric groups were 1.96 (1.15) *versus* 0.29 (0.40) (ADNI, $p < 0.001$) and 1.79 (1.13) *versus* 0.59 (0.49) (SMS, $p < 0.001$), respectively.

3.1. Findings from the ADNI cohort

3.1.1. Baseline characteristics of patients with asymmetric and symmetric tau distribution

Compared to patients with symmetric tau distribution, those with asymmetric tau pattern were characterized by a younger age at onset ($p = 0.017$), a higher proportion of EOAD ($p = 0.093$), and a younger age at baseline ($p = 0.006$). No significant intergroup differences were observed in terms of sex, education (years), disease duration, APOE ε4 status, and proportion of patients with MCI due to AD (all $p > 0.15$). In addition, the asymmetric group showed worse global cognition than symmetric group based on Montreal Cognitive Assessment (MOCA) scores ($p = 0.015$). No significant differences were observed on other neuropsychological tests (Table 2**,** Supplementary Table 3).

Cross-sectional comparisons between asymmetric and symmetric

Table 2
Demographic and clinical data of patients with asymmetric *versus* symmetric tau distribution in the ADNI (^{18}F-Flortaucipir) cohort.

	Cross-sectional (n = 60)			*Longitudinal (n = 39)*		
	Asymmetric tau distribution (n = 14)	*Symmetric tau distribution (n = 46)*	*p value*	*Asymmetric tau distribution (n = 9)*	*Symmetric tau distribution (n = 30)*	*p value*
Age at baseline (years)	*72.4 ± 9.0*	*79.2 ± 7.4*	*0.006a***	*69.8 ± 10.5*	*79.5 ± 5.7*	*0.025a***
Female/ Male (Female, %)	*7/7 (50.0%)*	*17/29 (37.0%)*	*0.383b*	*4/5 (44.4%)*	*11/19 (36.7%)*	*0.674b*
Education (years)	*14.6 ± 2.2*	*15.7 ± 2.5*	*0.152a*	*15.0 ± 1.7*	*15.6 ± 2.5*	*0.537a*
APOE ε4-positive/negative (positive, %) [1]	*9/5 (64.3%)*	*26/19 (57.8%)*	*0.261c*	*6/3 (66.7%)*	*18/11 (62.1%)*	*0.840c*
MCI/AD (MCI, %)	*8/6 (57.1%)*	*33/13 (71.7%)*	*0.308c*	*2/7 (22.2%)*	*13/17 (43.3%)*	*0.348c*
Age at onset (years)	*65.9 ± 7.4*	*71.4 ± 7.3*	*0.017a**	*63.7 ± 7.7*	*71.9 ± 6.0*	*0.002a***
EOAD/LOAD (EOAD, %)	*5/9 (35.7%)*	*7/39 (15.2%)*	*0.093b*	*4/5 (44.4%)*	*3/27 (10.0%)*	*0.018b**
Disease duration at baseline (years)	*6.4 ± 4.0*	*7.8 ± 4.8*	*0.352a*	*6.8 ± 4.8*	*7.7 ± 4.0*	*0.581a*
Baseline-last visit interval (years)	*/*	*/*	*/*	*1.3 ± 0.5*	*1.8 ± 0.9*	*0.177a*
MMSE at baseline	*21.3 ± 5.5*	*23.9 ± 4.6*	*0.126d*	*20.9 ± 6.2*	*25.0 ± 3.4*	*0.009d***
MMSE at last visit [2]	*/*	*/*	*/*	*15.8 ± 7.3*	*22.6 ± 4.9*	*0.013d**
MOCA at baseline	*14.3 ± 6.2*	*19.0 ± 5.2*	*0.015d**	*14.0 ± 6.9*	*19.4 ± 5.0*	*0.035d**
MOCA at last visit [2]	*/*	*/*	*/*	*13.6 ± 6.8*	*19.4 ± 6.8*	*0.002d***
CDRSB at baseline	*5.2 ± 3.8*	*4.4 ± 3.6*	*0.279d*	*5.0 ± 4.4*	*3.5 ± 2.6*	*0.019d**
CDRSB at last visit [2]	*/*	*/*	*/*	*8.2 ± 3.7*	*5.5 ± 4.3*	*0.084d*
FAQ at baseline	*12.9 ± 9.6*	*11.7 ± 9.2*	*0.401d*	*11.6 ± 9.9*	*9.8 ± 8.1*	*0.141d*
FAQ at last visit [2]	*/*	*/*	*/*	*18.9 ± 7.6*	*12.1 ± 10.5*	*0.072d*
RCD/NCD (RCD, %)	*/*	*/*	*/*	*2/7 (22.2%)*	*2/28 (6.7%)*	*0.387e*

Data are presented as mean ± standard deviation unless otherwise specified.
a. Student's *t*-test. b. Chi-square test. c. Mann-Whitney *U* test. d. Generalized linear model adjusted for age and disease duration at baseline, education (years), APOE ε4 status, and sex. e. Generalized linear model adjusted for age and disease duration at baseline, education (years), APOE ε4 status, sex, and MMSE score at baseline.
*, $p < 0.05$; **, $p < 0.01$.
Abbreviations: ADNI, Alzheimer's Disease Neuroimaging Initiative; APOE, Apolipoprotein E; MCI, mild cognitive impairment; AD, Alzheimer's disease; EOAD, early-onset AD; LOAD, late-onset AD; MMSE, Mini-Mental Status Examination; MOCA, Montreal Cognitive Assessment; CDRSB, Clinical Dementia Rating, Sum of Boxes; FAQ, Functional Assessment Questionnaire; RCD, Rapid cognitive decline; NCD, Normal rate of cognitive decline.
[1] The presence of at least one APOE ε4 allele was regarded as APOE ε4-positivity. Data on the APOE genotype were missing for one patient.
[2] Neuropsychological results were partially missing at the last visit for some patients. MMSE, CDRSB, and FAQ scores were missing for one patient in the symmetric group. The MOCA scores were available for 5 and 23 patients in the asymmetric and symmetric groups, respectively.

groups revealed that the former harbored more severe tau [median (interquartile range) of global SUVR: 1.61 (0.29) *versus* 1.27 (0.18), $p < 0.001$; Fig. 1**B**] and amyloid [median (interquartile range) of global SUVR: 1.62 (0.30) *versus* 1.39 (0.28), $p = 0.015$; Fig. 1**C**] burdens.

3.1.2. Longitudinal cognitive decline in patients with asymmetric and symmetric tau distribution

Nine (64.3%) and 30 (65.2%) patients who showed an asymmetric *versus* symmetric tau distribution underwent at least one follow-up examination after baseline PET tau imaging (mean time interval from the scan: 1.6 years, standard deviation: 0.8 years). The clinical profiles are presented in Table 2. After adjustment for age at baseline, education (years), APOE ε4 status, and sex, LMEM analyses identified a less favorable prognosis in patients with asymmetric tau distribution **(**Fig. 2A, Supplementary Table 4**)**. A more rapid cognitive deterioration (annual difference: β ± SE) was observed for the MMSE (-0.92 ± 0.46, $p = 0.053$), Alzheimer's Disease Assessment Scale (11 items, ADAS11; 1.82 ± 0.87, $p = 0.041$), Clinical Dementia Rating (Sum of Boxes, CDRSB; 0.79 ± 0.35, $p = 0.030$), and Functional Assessment Questionnaire (FAQ; 2.42 ± 0.83, $p = 0.005$) scores. When further adjusted for EOAD/LOAD, the longitudinal cognitive declines reflecting by all above neuropsychological tests did not appreciably change (Supplementary Table 4).

3.2. Findings from the SMS cohort

3.2.1. Baseline characteristics of patients with asymmetric and symmetric tau distribution

The cross-sectional findings in the SMS cohort were generally consistent with those observed in the ADNI cohort. First, we found a higher proportion of EOAD in the asymmetric group ($p = 0.026$). No significant difference was seen on age at baseline ($p = 0.281$) and age at onset ($p = 0.325$). Similarly, there were no significant differences in terms of sex, education (years), disease duration, APOE ε4 status, and proportion of MCI patients (all $p > 0.35$). As for cognitive function, no obvious differences were found between the two groups (all $p > 0.15$; Table 3, Supplementary Table 3). On analyzing PET biomarkers (Fig. 1E-F), the asymmetric group suffered from a more severe "T" burden than the symmetric group [median (interquartile range) of global SUVR: 1.55 (0.47) *versus* 1.30 (0.46), $p = 0.007$], while no significant intergroup difference was found in amyloid burden [median (interquartile range) of global SUVR: 1.42 (0.16) *versus* 1.39 (0.27), $p = 0.662$]. Meanwhile, comparison of blood biomarkers between asymmetric and symmetric groups showed a consistent finding in "T" burden and a similar trend in "A" burden: median (interquartile range) of p-tau 181 levels: 5.10 (2.33) *versus* 4.11 (1.91) pg/mL, $p = 0.007$; median (interquartile range) of P-tau181/Aβ42 ratio: 0.06 (0.27) *versus* 0.47 (0.15), $p < 0.001$; mean ± standard deviation of Aβ42/Aβ40 ratio: 0.048 ± 0.012 *versus* 0.050 ± 0.012, $p = 0.546$ (Fig. 3). No significant intergroup differences in plasma biomarkers of neurodegeneration were observed [median (interquartile range) of T-tau: 2.88 (2.01) *versus* 3.13 (3.08) pg/mL, $p = 0.946$; and NfL: 19.07 (7.09) *versus* 17.12 (6.11) pg/mL, $p = 0.628$].

3.2.2. Longitudinal cognitive decline in patients with asymmetric and symmetric tau distribution

Twenty-six (61.9%) and 26 (57.8%) patients who showed an asymmetric *versus* symmetric tau distribution underwent at least one clinical follow-up visit and neuropsychological testing after baseline PET imaging (mean time interval from the scan: 1.2 years, standard deviation: 0.8 years). The patient clinical profiles are presented in Table 3. On applying LMEM analyses, we found that the difference of slope of longitudinal cognitive decline was similar to that observed in the ADNI cohort in terms of global cognition and language function (Fig. 2B, Supplementary Table 4). Patients with asymmetric tau distribution declined more rapidly than those with a symmetric distribution with respect to the following tests or domains (annual difference: β ± SE):

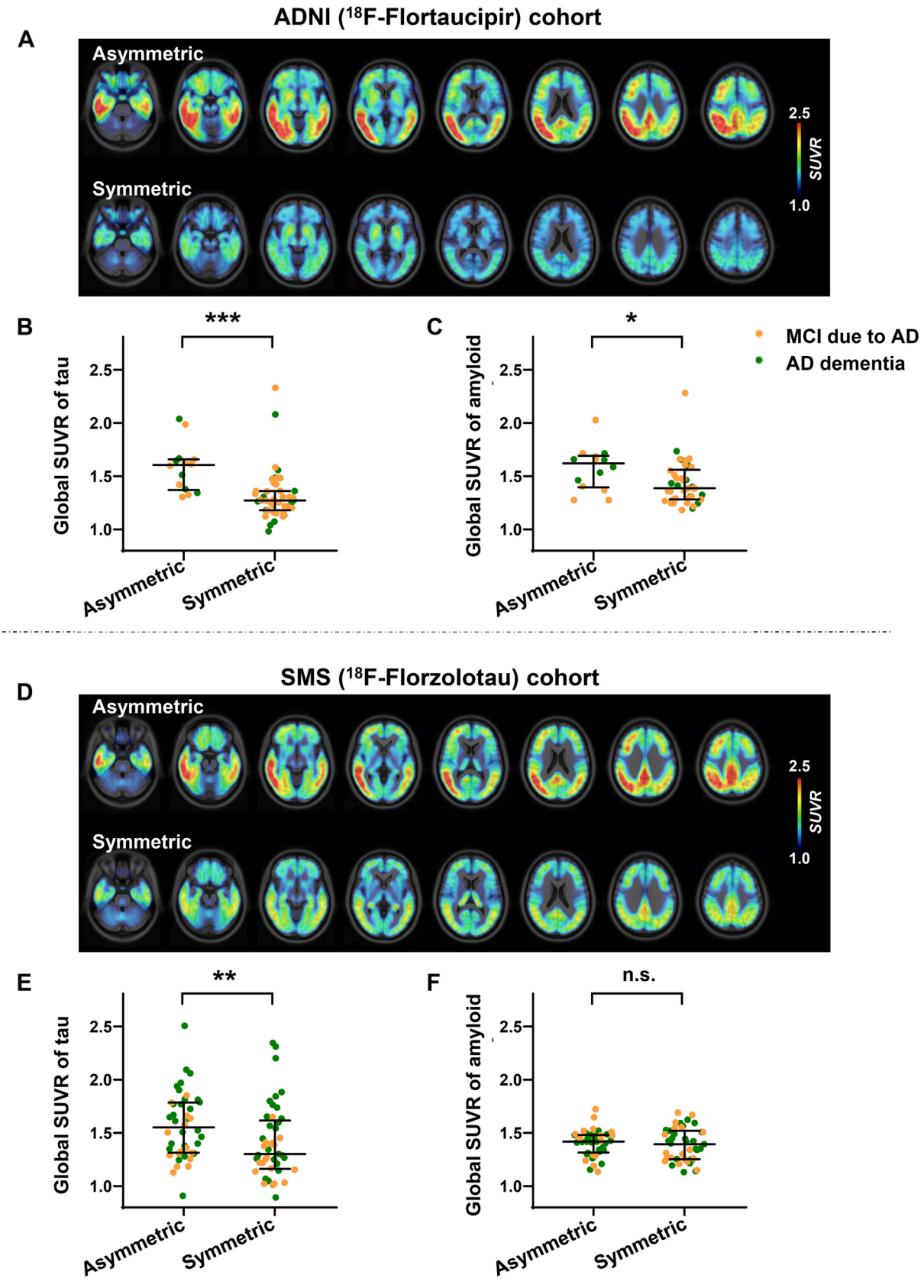

(caption on next page)

Fig. 1. Differences in "A/T" burden in patients with asymmetric *versus* symmetric tau distribution on PET images. (A) Average tau SUVR PET images in patients with asymmetric *versus* symmetric tau distribution in the ADNI cohort. In presence of an asymmetric tau distribution, images of patients with a left asymmetry were flipped on the X-axis, whereas images of patients with a symmetric tau distribution were randomly flipped on the X-axis. **(B-C)** In the ADNI cohort, the global tau and amyloid burden was investigated using ^{18}F-Flortaucipir PET and ^{18}F-Florbetapir PET imaging, respectively. Three patients whose amyloid PET imaging was performed not during the same period of their tau PET scan were excluded from the comparison of amyloid burden. **(D)** Average tau SUVR PET images in patients with asymmetric *versus* symmetric tau distribution in the SMS cohort. The methodology was identical to that implemented in the ADNI cohort. **(E-F)** In the SMS cohort, the global tau and amyloid burden was investigated using ^{18}F-Florzolotau PET and ^{18}F-Florbetapir PET imaging. Four patients with ^{11}C-PIB amyloid PET imaging were excluded from comparisons of the amyloid burden. *, $p < 0.05$; **, $p < 0.01$; ***, $p < 0.001$; n.s., not significant; Mann-Whitney *U* test. The error bars represent the median (interquartile range). Abbreviations: ADNI, Alzheimer's Disease Neuroimaging Initiative; SMS, Shanghai Memory Study; SUVR, standardized uptake value ratio; MCI, mild cognitive impairment; AD, Alzheimer's disease.

MMSE: -1.16 ± 0.51, $p = 0.035$; Boston Naming Test (BNT): -2.12 ± 0.74, $p = 0.008$. Albeit not statistically significant, the asymmetric group also showed a trend toward a less favorable global cognition (MOCA: -0.94 ± 0.54, $p = 0.097$), instrumental activities of daily living function (FAQ: 0.99 ± 0.55, $p = 0.084$). No other differences in neuropsychological testing were observed (all $p > 0.25$). When further adjusted for EOAD/LOAD, the results remained similar (Supplementary Table 4). Notably, a higher proportion of RCD was observed in the asymmetric group (30.8% *versus* 7.7%, $p = 0.027$).

3.3. Findings from the combined cohort

The calculation of standardized Z-scores (*abs*GAS) in the asymmetric and symmetric groups allowed merging the ADNI and SMS cohorts into a unique group for additional analysis. Consistently, patients with asymmetric tau distribution had a higher percentage of EOAD (53.6% *versus* 28.4%, $p = 0.001$), along with younger age at onset (mean ± standard deviation: 63.6 ± 10.1 *versus* 68.2 ± 9.3, $p = 0.004$) and age at baseline (mean ± standard deviation: 66.8 ± 10.1 *versus* 73.3 ± 10.4, $p < 0.001$). While the global cognitive function and functional impairment in daily living were similar between the two groups (all $p > 0.7$), patients with asymmetric tau distribution had a higher percentage of RCD (28.9% *versus* 7.1%, $p = 0.004$). In the asymmetric group, the results of LMEM consistently revealed a rapid cognitive decline according to MMSE ($\beta \pm SE = -1.46 \pm 0.34$, $p < 0.001$), MOCA ($\beta \pm SE = -1.31 \pm 0.36$, $p < 0.001$), CDRSB ($\beta \pm SE = 0.55 \pm 0.22$, $p = 0.017$), and FAQ ($\beta \pm SE = 1.77 \pm 0.48$, $p < 0.001$; Fig. 2**C**) scores. When further adjusted for EOAD/LOAD, the results did not appreciably change (Supplementary Table 4).

3.4. Comparison between patients with left- and right-predominant asymmetric tau distribution

As the sample size in the ADNI cohort was limited and cognitive data with respect to specific domains were unavailable, the exploratory comparisons between left- and right-predominant asymmetric tau distribution subgroups were performed in the SMS cohort only. Of the 42 patients with asymmetric tau deposition, 22 (52.4%) and 20 (47.6%) were left- and right-predominant, respectively. While no significant differences were observed in terms of demographic characteristics, cognition, and measures of "A/T" pathology, the left-predominant group showed more severe neurodegeneration [median (interquartile range) of plasma T-tau: 3.30 (2.38) *versus* 2.34 (2.30) pg/mL, $p = 0.096$; plasma NfL: 20.59 (11.95) *versus* 17.00 (6.77) pg/mL, $p = 0.032$; Supplementary Table 5).

4. Discussion

This study, conducted in two ethnically diverse, independent cohorts, has three principal findings. First, we confirmed that an asymmetric tau distribution is existed in patients with AD. Second, compared with patients with symmetric tau distribution, those with an asymmetric tau distribution were characterized by an earlier disease onset, and a more severe AD-related pathological burden. Third, the presence of asymmetric tau deposits was associated with a more rapid cognitive decline. Collectively, these findings provide initial evidence that the asymmetric tau distribution on PET may be one of the hallmarks of AD heterogeneity worthy of in-depth investigation. For further application, more comprehensive evaluation and validation of the different asymmetry indicators, and the investigation on the underlying mechanisms are imperative.

AD is conceptualized as a neurodegenerative disease spectrum with substantial phenotypic heterogeneity (Vogel et al., 2021). Within the non-linear dynamic continuum of AD pathophysiology, an asymmetric pathology is most commonly observed in atypical AD (Gefen et al., 2012; Lehmann et al., 2013; Nasrallah et al., 2018; Ohm et al., 2020; Tetzloff et al., 2018), which is characterized by accelerated and more severe clinical manifestations within common AD subtypes (Vogel et al., 2021). Recently, such uneven involvement was also revealed in certain patients with typical AD (Frings et al., 2015; Vogel et al., 2021; Weise et al., 2018; Yoon et al., 2021). However, previous investigations were chiefly focused on amyloid depositions or neurodegeneration. In this scenario, the clinical and prognostic relevance of asymmetric tau distribution has not been entirely elucidated. In this study, we investigated the unbalanced tau deposition on tau PET imaging within pathologically confirmed (A +) patients with MCI and AD dementia, and found asymmetry in some subjects. Our results were in line with those of two recent studies where the asymmetric temporoparietal involvement / medial temporal lobes involvement on ^{18}F-Flortaucipir tau PET imaging was identified as the distinct trajectories of tau deposition associated with specific clinical phenotypes in patients with AD / individual with preclinical AD (Vogel et al., 2021; Young et al., 2022). Notably, an asymmetric pathological pattern can be universally found in other neurodegenerative disorders – including FTLD (Bang et al., 2015) and CBD (Di Stasio et al., 2019). The relatively strict inclusion criteria (all patients were "A+") applied in current study and the exclusive exclusion of patients with clinically atypical AD in the SMS cohort allowed us to reduce the amount of confounding and increase the reliability of our conclusions. The exclusion of atypical AD in the SMS (^{18}F-Florzolotau) cohort could partly underestimate the rate of asymmetric tau pattern in the entire AD spectrum. Surprisingly, the proportion of patients with asymmetric tau distribution in the SMS (^{18}F-Florzolotau) cohort was higher than that observed in the ADNI (^{18}F-Flortaucipir) cohort (48.3% *versus* 23.3%). This difference may be related to the younger age at onset (EOAD%: 47.1% *versus* 20.0%) and the more advanced disease stages (AD dementia%: 62.1% *versus* 31.7%) in the SMS (^{18}F-Florzolotau) cohort; in this regard, more aggressive variants can enhance the expression of specific subtypes (Vogel et al., 2021). Alternatively, we cannot rule out the possibility that the occurrence of the asymmetric tau pattern could have been underestimated in the ADNI cohort. Although both ^{18}F-Flortaucipir and ^{18}F-Florzolotau are targeted to pathological tau, they have different binding properties, that is, the former used in the ADNI cohort has a high sensitivity to paired helical filaments (PHFs) but its affinity to 4R-tau is limited (Marquié et al., 2017), whereas the latter applied to the SMS cohort has showed the high affinity to both PHFs and 4R-tau deposits (Tagai et al., 2021).

Our results obtained in two independent, ethnically diverse cohorts support the notion that an asymmetric tau distribution on PET imaging may be an important clue to an earlier age at onset and a more severe pathological burden. An earlier age at onset in AD has been associated

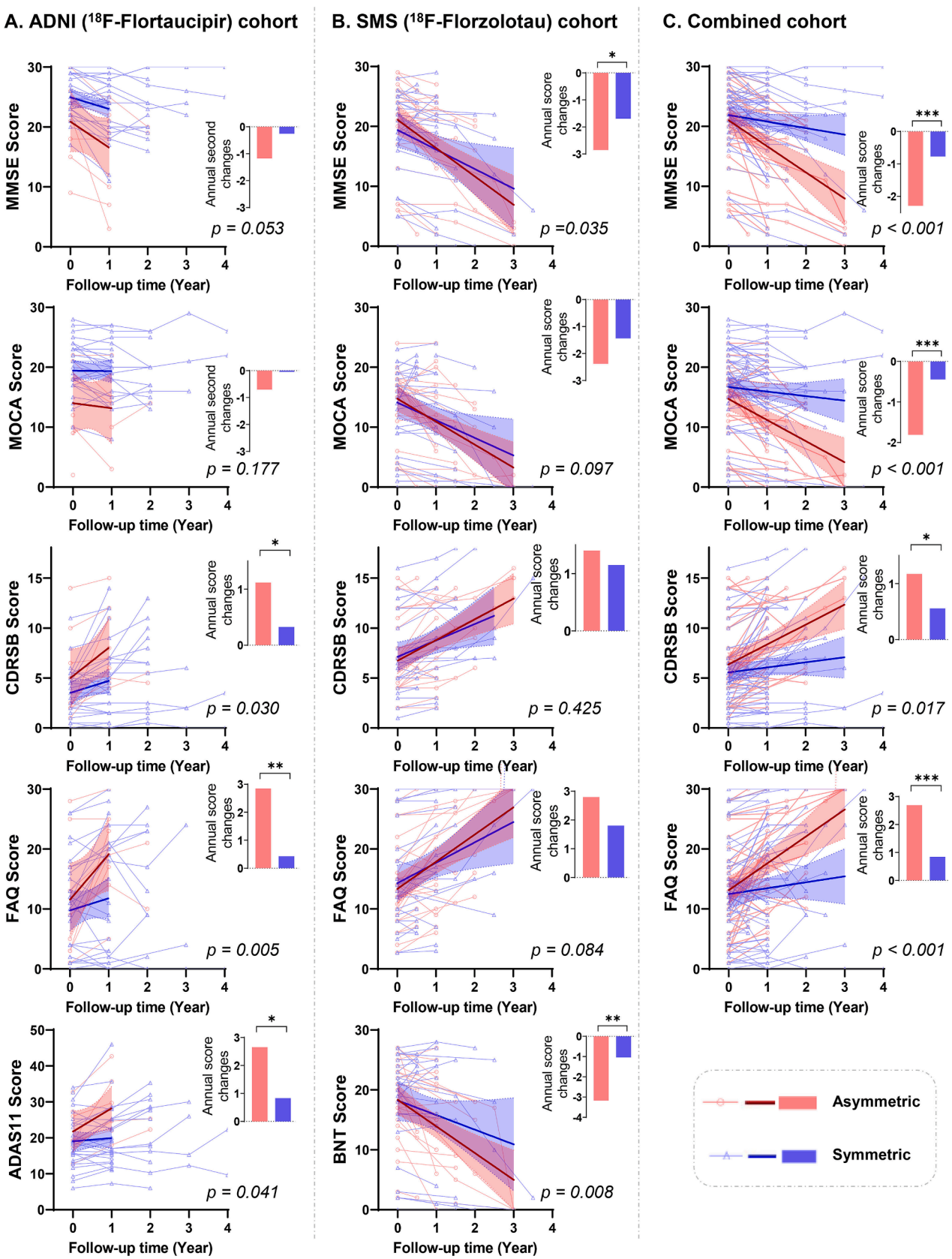

(caption on next page)

Fig. 2. Raw scores and estimated annual changes on neuropsychological testing over time in patients with asymmetric *versus* symmetric tau distribution. The compound figures consisted of raw spaghetti plots with separate lines showing the unadjusted mean trajectory (with its 95% confidence interval) and the estimated annual changes after adjusting for age at baseline, education (years), APOE ε4 status, and sex for each cohort **(A-B)**. Different cohort was further adjusted when analyzing the combined cohort **(C)**. The spaghetti plots depict the raw scores on neuropsychological tests administered at each visit; the separate lines denote the unadjusted mean trajectory (with its 95% confidence interval) of patients with asymmetric *versus* symmetric tau distribution. In the ADNI cohort, limited data were available for the last three visits (asymmetric tau distribution: n = 2, 0, 0; symmetric tau distribution: n = 10, 4, 2). Similarly, data concerning the last two visits were limited in the SMS cohort (asymmetric tau distribution: n = 0, 0; symmetric tau distribution: n = 1, 2). Therefore, lines were generated after their exclusion. The bar charts show the estimated annual changes of scores on neuropsychological tests. The p values are calculated for the differences in the slope of longitudinal decline between patients with asymmetric *versus* symmetric tau distribution using a linear mixed-effect model adjusted for age at baseline, education (years), APOE ε4 status, and sex for each cohort; disease duration was considered as a time scale. Different cohort was further adjusted when analyzing the combined cohort. *, $p < 0.05$; **, $p < 0.01$; ***, $p < 0.001$. Abbreviations: ADNI, Alzheimer's Disease Neuroimaging Initiative; SMS, Shanghai Memory Study; MMSE, Mini-Mental Status Examination; MOCA, Montreal Cognitive Assessment; CDRSB, Clinical Dementia Rating, Sum of Boxes; FAQ, Functional Assessment Questionnaire; ADAS11, Alzheimer's Disease Assessment Scale (11 items); BNT, Boston Naming Test.

Table 3
Demographic and clinical data of patients with asymmetric *versus* symmetric tau distribution in the SMS (^{18}F-Florzolotau) cohort.

	Cross-sectional (n = 87)			*Longitudinal (n = 52)*		
	Asymmetric tau distribution (n = 42)	*Symmetric tau distribution (n = 45)*	*p value*	*Asymmetric tau distribution (n = 26)*	*Symmetric tau distribution (n = 26)*	*p value*
Age at baseline (years)	*65.0 ± 9.9*	*67.2 ± 9.5*	*0.281a*	*63.2 ± 9.6*	*66.9 ± 10.9*	*0.191a*
Female/ Male (Female, %)	*26/16 (61.9%)*	*32/13 (71.1%)*	*0.363b*	*15/11 (57.7%)*	*17/9 (65.4%)*	*0.569b*
Education (years)	*10.3 ± 3.5*	*10.3 ± 4.0*	*0.997a*	*9.9 ± 3.7*	*11.2 ± 4.0*	*0.239a*
APOE ε4-positive/negative (positive, %) [1]	*26/15 (63.4%)*	*30/15 (66.7%)*	*0.753c*	*13/12 (52.0%)*	*17/9 (65.4%)*	*0.266c*
MCI/AD (MCI, %)	*15/27 (35.7%)*	*18/27 (40.0%)*	*0.682c*	*8/18 (30.8%)*	*8/18 (30.8%)*	*1.000c*
Age at onset (years)	*62.8 ± 10.3*	*64.9 ± 10.0*	*0.325a*	*60.5 ± 9.7*	*64.2 ± 11.3*	*0.217a*
EOAD/LOAD (EOAD, %)	*25/17 (59.5%)*	*16/29 (35.6%)*	*0.026b**	*19/6 (76.0%)*	*11/14 (44.0%)*	*0.021b**
Disease duration at baseline (years)	*2.2 ± 2.0*	*2.3 ± 1.9*	*0.811a*	*2.6 ± 2.1*	*2.8 ± 2.2*	*0.745a*
Baseline-last visit interval (years)	/	/	/	*1.2 ± 0.8*	*1.1 ± 0.8*	*0.629a*
MMSE at baseline	*20.7 ± 6.5*	*20.2 ± 6.6*	*0.296d*	*20.2 ± 7.0*	*18.7 ± 7.6*	*0.032d**
MMSE at last visit	/	/	/	*15.8 ± 8.5*	*16.8 ± 9.0*	*0.850d*
MOCA at baseline	*14.6 ± 5.6*	*13.7 ± 6.4*	*0.160d*	*14.2 ± 5.8*	*12.8 ± 7.0*	*0.018d**
MOCA at last visit	/	/	/	*10.3 ± 7.3*	*12.2 ± 8.3*	*0.812d*
CDRSB at baseline	*7.0 ± 3.4*	*6.9 ± 3.5*	*0.878d*	*7.1 ± 3.8*	*7.4 ± 3.9*	*0.416d*
CDRSB at last visit	/	/	/	*9.1 ± 4.1*	*8.8 ± 4.6*	*0.995d*
FAQ at baseline	*14.3 ± 6.4*	*14.3 ± 7.4*	*0.594d*	*14.2 ± 7.1*	*15.2 ± 8.5*	*0.080d*
FAQ at last visit	/	/	/	*18.3 ± 8.5*	*17.0 ± 9.4*	*0.886d*
RCD/NCD (RCD, %)	/	/	/	*8/18 (30.8%)*	*2/24 (7.7%)*	*0.027e**

Data are presented as mean ± standard deviation unless otherwise specified.
a. Student's *t*-test. b. Chi-square test. c. Mann-Whitney *U* test. d. Generalized linear model adjusted for age and disease duration at baseline, education (years), APOE ε4 status, and sex. e. Generalized linear model adjusted for age and disease duration at baseline, education (years), APOE ε4 status, sex, and MMSE score at baseline.
*, $p < 0.05$.
Abbreviations: SMS, Shanghai Memory Study; APOE, Apolipoprotein E; MCI, mild cognitive impairment; AD, Alzheimer's disease; EOAD, early-onset AD; LOAD, late-onset AD; MMSE, Mini-Mental Status Examination; MOCA, Montreal Cognitive Assessment; CDRSB, Clinical Dementia Rating, Sum of Boxes; FAQ, Functional Assessment Questionnaire; RCD, Rapid cognitive decline; NCD, Normal rate of cognitive decline.
[1] The presence of at least one APOE ε4 allele was regarded as APOE ε4-positivity. Data on the APOE genotype were missing for one patient.

with atypical clinical symptoms (*i.e.*, behavioral manifestations), non-memory impairment, rapid disease progression, more severe pathological tau burden (Cho et al., 2017; Marshall et al., 2007) and relatively atypical pathological tau distribution (Murray et al., 2011; Vogel et al., 2021). Here, we found that an asymmetric tau pattern was associated with the clinical and pathological features of early-onset AD. It's worth noting that the more severe amyloid burden in the asymmetric group compared with the symmetric group was observed in the ADNI cohort by amyloid PET, while in the SMS cohort, it was only found significant in plasma P-tau181/Aβ42 ratio, a biomarker which was recently reported to outperform plasma Aβ42/Aβ40 ratio in differentiating A + AD from A- subjects (Chong et al., 2021). The higher proportion of MCI due to AD in the ADNI cohort than the SMS cohort may help to explain given that the amyloid accumulation would reach a plateau earlier than tau (Aisen et al., 2017). Given the difference in the composition of participants between the cohorts in our research, future validation in subjects with similar enrollment is necessary. In addition to "A/T" burden, changes in "N" were also compared via plasma T-tau and NfL levels between the asymmetric and symmetric groups in the SMS cohort. The insignificant differences in these "N" biomarkers may be because of their low specificity of AD neuropathology (Smirnov et al., 2022). Of note, asymmetry in amyloid deposition was previously reported to be clinically relevant, which was consistent with our findings (Frings et al., 2015; Yoon et al., 2021). However, considering the different spatiotemporal trajectories of amyloid and tau during the progression of AD (Goedert, 2015), the association between their asymmetries remains to be explored. Further studies encompassing the asymmetric distribution throughout the entire "A/T/N" pathological framework are warranted.

On analyzing the prognostic significance of asymmetric tau distribution, we found this PET imaging feature predicted a steeper cognitive decline over time. Brain asymmetries have been previously implicated in human cognition by affecting the functional network organization (Postema et al., 2019; Wang et al., 2014). Roe et al. (2021) demonstrated that asymmetric thinning of the cerebral cortex occurs during normal aging and is accelerated in AD. Yoon et al. (2021) have also recently reported that asymmetric amyloid deposition on PET images may serve as an early sign of progression in MCI and AD. In light of the anatomical overlaps between the occurrence of cortical thinning and tau deposition in AD (Jagust, 2018), we found that asymmetric tau deposition was associated with a more rapid cognitive decline over time in two independent cohorts – despite the differences of baseline characteristics in cognitive function. Given that the proportion of EOAD might confound the between-group differences, the subgroup of EOAD and LOAD was also included as a covariate in the longitudinal analysis, and the more rapid cognitive decline remained significant in the asymmetric group compared with the symmetric group. Our study confirms and expands

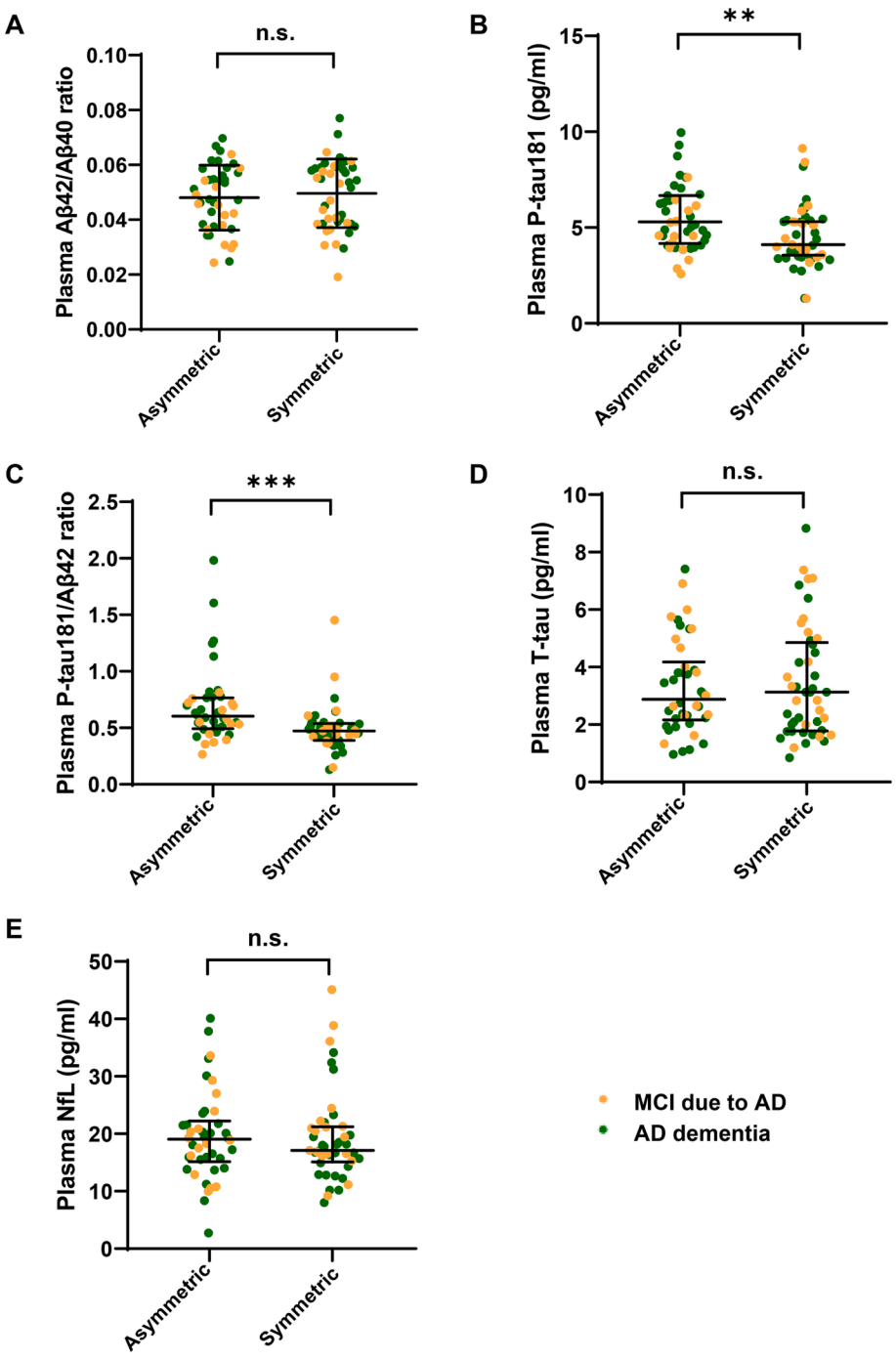

Fig. 3. Plasma biochemical markers of the "A/T/N" classification system in patients with asymmetric *versus* symmetric tau distribution in the SMS (^{18}F-Florzolotau) cohort. **, $p < 0.01$; ***, $p < 0.001$; n.s., not significant; Student's *t*-test for plasma Aβ42/Aβ40 ratio, and Mann-Whitney *U* test for others. The error bars represent the mean (standard deviation) for plasma Aβ42/ Aβ40 ratio, and median (interquartile range) for others. Abbreviations: MCI, mild cognitive impairment; AD, Alzheimer's disease; Aβ, amyloid-beta protein; P-tau181, tau phosphorylated at threonine 181; T-tau, total tau; NfL, neurofilament protein light chain.

previous observations on the potential value of tau PET imaging in predicting the progression of cognitive decline within the AD spectrum (Jack et al., 2020; Joie et al., 2020). Subject to future confirmation, the unfavorable prognostic value of an asymmetric tau deposition may have a significant translational impact in terms of therapeutic interventions, planning for care, and other dimensions related to disease management.

The mechanisms underlying the asymmetric *versus* symmetric tau distribution deserve further investigation. Complex genetic and epigenetic factors are likely to play a role as they have been shown to influence age-related brain changes (Fjell et al., 2015), cortical thickness asymmetry (Li et al., 2015), brain development (Ziffra et al., 2021) and age-related diseases (Mc Auley, 2021). Notably, a study conducted in PD has shown that divergent neuronal epigenetic patterns are associated with its hemispheric asymmetry (Li et al., 2020). In the current study, the APOE ε4 allele was not found to affect asymmetric *versus* symmetric tau distribution in AD. While this may be explained by the relatively minor role played by the APOE ε4 allele in EOAD (Smirnov et al., 2021), the possibility that the sample size may not have been sufficiently large to identify significant differences should not be excluded. Future genome-wide studies in the field of imaging genetics – exploring how genetic and epigenetic risk factors may affect brain imaging findings – will be required to analyze and characterize intermediate biological phenotypes responsible for the differences in tau lateralization within the AD spectrum. While sex and education are also known to influence AD heterogeneity, they were not found to influence tau distribution in the current study. Besides, the molecular diversity of tau, which associates with differences in aggressiveness of clinical course in AD (Dujardin et al., 2020) may also help to explain, although detection of

different tau forms *in vivo* remains challenging.

Even though the sample size in each subgroup was small, we divided patients with an asymmetric tau distribution in the SMS cohort according to their left- *versus* right-predominance. No significant difference was observed in terms of demographic characteristics or cognitive performances; however, more severe neurodegeneration (plasma t-tau and NfL) was observed in the patients with left-predominance. Cognitive processing – including language and visuospatial functioning – is deemed to show hemispheric dominance. Our data concerning the lack of differences in cognitive performance should be considered preliminary and warrants further confirmation. Similarly, the occurrence of more severe neurodegeneration in patients with left-predominance deserves further scrutiny because of the limited sample size.

There are limitations to this study. First, the two cohorts differed in the proportion of patients with MCI due to AD – which limited the ability to further compare the baseline cognitive characteristics between the ADNI and SMS cohorts. Meanwhile, although the current study focused on typical AD, we could not rule out atypical AD, if any, in the ADNI cohort due to the lack of detailed information on clinical phenotype. Second, HCs in the SMS cohort were younger than patients. While a previous study has shown that ^{18}F-Florzolotau uptake did not correlate with age in HCs (Li et al., 2021), further research with a larger sample size of age-matched controls is necessary to confirm our data. Besides, other demographic mismatches between patients and controls also warranted attention. Validation in large-scale studies with matched HCs should be scheduled. Third, the limited sample size precluded additional comparisons of patients according to their left- *versus* right-predominance, as well as separate analysis of MCI due to AD and AD dementia. Fourth, it is also possible that the sample size may have not been sufficiently large (in terms of study power) to identify an impact of the APOE ε4 allele, sex, and education on asymmetric *versus* symmetric tau distribution and, for that reason, larger prospective cohorts are needed. Fifth, the sample size for the longitudinal study and the follow-up time were limited. Sixth, as we had no longitudinal imaging data, we were unable to track the dynamic changes of asymmetric tau distribution occurring over time. Seventh, the interval between tau PET imaging, structural MRI, and neuropsychological testing may affect the consistency of clinical symptoms and pathological burden. Finally, our study was not specifically designed to identify the biological mechanisms responsible for an asymmetric *versus* symmetric tau distribution. Future imaging genetics studies aimed at exploring how genetic factors correlate with PET tau imaging findings should work to address this caveat.

5. Conclusions

The current study demonstrates that asymmetric tau distribution represents an important feature of AD heterogeneity. Albeit preliminary, our results suggest that an asymmetric pattern on tau PET imaging identifies a subgroup of patients with an earlier disease at onset and a more aggressive clinical course in terms of cognitive decline.

Funding

This work was supported by the National Natural Science Foundation of China (grants 81971641, 82071200, 82021002, 82272039), the National Project of Chronic Disease of China (grant 2016YFC1306402), the Shanghai Aging and Maternal and Child Health Research Special Project (grant 2020YJZX0111), the Clinical Research Plan of Shanghai Hospital Development Center (grants SHDC2020CR1038B and SHDC2020CR4007), the China Scholarship Council (grant 202006100181), the Science and Technology Innovation 2030 Major Project (grant 2022ZD0211600), the National Key R&D Program of China (grants 2022YFC2009902, 2022YFC2009900).

CRediT authorship contribution statement

Jiaying Lu: Conceptualization, Methodology, Software, Formal analysis, Investigation, Resources, Data curation, Writing – original draft, Visualization, Funding acquisition. **Zhengwei Zhang:** Methodology, Validation, Investigation, Writing – original draft. **Ping Wu:** Investigation, Writing – review & editing. **Xiaoniu Liang:** Investigation, Writing – review & editing. **Huiwei Zhang:** Investigation, Writing – review & editing. **Jimin Hong:** Software, Writing – review & editing. **Christoph Clement:** Software, Writing – review & editing. **Tzu-Chen Yen:** Writing – review & editing. **Saineng Ding:** Investigation, Writing – review & editing. **Min Wang:** Software, Validation, Writing – review & editing. **Zhenxu Xiao:** Investigation, Writing – review & editing. **Axel Rominger:** Writing – review & editing. **Kuangyu Shi:** Writing – review & editing. **Yihui Guan:** Conceptualization, Investigation, Resources, Data curation, Writing – review & editing, Supervision, Project administration. **Chuantao Zuo:** Conceptualization, Investigation, Resources, Data curation, Writing – review & editing, Supervision, Project administration, Funding acquisition. **Qianhua Zhao:** Conceptualization, Investigation, Resources, Data curation, Writing – review & editing, Supervision, Project administration, Funding acquisition.

Declaration of Competing Interest

The authors declare the following financial interests/personal relationships which may be considered as potential competing interests: Tzu-Chen Yen is an employee of APRINOIA Therapeutics Co., Ltd (Suzhou, China). Axel Rominger and Kuangyu Shi have received research support from Novartis and Siemens Healthineers. All authors have no conflicts of interest regarding this manuscript.

Data availability

Data will be made available on request.

Acknowledgements:

The authors thank the patients and family members who participated in the research both from Huashan Hospital and the ADNI database. We are grateful to APRINOIA Therapeutics Co., Ltd (Suzhou, China) for providing the tosylate precursor used for ^{18}F-Florzolotau radiosynthesis.

Data from the Alzheimer's Disease Neuroimaging Initiative (ADNI) database (available at https://adni.loni.usc.edu) was funded by the ADNI (National Institutes of Health Grant U01 AG024904) and DOD ADNI (Department of Defense award number W81XWH-12-2-0012). ADNI is funded by the National Institute on Aging, the National Institute of Biomedical Imaging and Bioengineering, and through generous contributions from the following sources: AbbVie, Alzheimer's Association; Alzheimer's Drug Discovery Foundation; Araclon Biotech; BioClinica, Inc.; Biogen; Bristol-Myers Squibb Company; CereSpir, Inc.; Cogstate; Eisai Inc.; Elan Pharmaceuticals, Inc.; Eli Lilly and Company; EuroImmun; F. Hoffmann-La Roche Ltd and its affiliated company Genentech, Inc.; Fujirebio; GE Healthcare; IXICO Ltd.; Janssen Alzheimer Immunotherapy Research & Development, LLC.; Johnson & Johnson Pharmaceutical Research & Development LLC.; Lumosity; Lundbeck; Merck & Co., Inc.; Meso Scale Diagnostics, LLC.; NeuroRx Research; Neurotrack Technologies; Novartis Pharmaceuticals Corporation; Pfizer Inc.; Piramal Imaging; Servier; Takeda Pharmaceutical Company; and Transition Therapeutics. The Canadian Institutes of Health Research is providing funds to support ADNI clinical sites in Canada. Private sector contributions are facilitated by the Foundation for the National Institutes of Health (www.fnih.org). The grantee organization is the Northern California Institute for Research and Education, and the study is coordinated by the Alzheimer's Therapeutic Research Institute at the University of Southern California. ADNI data are disseminated by the Laboratory for Neuro Imaging at the University of

Southern California.

Appendix A. Supplementary data

Supplementary data to this article can be found online at https://doi.org/10.1016/j.nicl.2023.103416.

References

Aisen, P.S., Cummings, J., Jack, C.R., Morris, J.C., Sperling, R., Frölich, L., Jones, R.W., Dowsett, S.A., Matthews, B.R., Raskin, J., Scheltens, P., Dubois, B., 2017. On the path to 2025: Understanding the Alzheimer's disease continuum. Alzheimer's Res. Ther. 9, 60. https://doi.org/10.1186/s13195-017-0283-5.

Albert, M.S., DeKosky, S.T., Dickson, D., Dubois, B., Feldman, H.H., Fox, N.C., Gamst, A., Holtzman, D.M., Jagust, W.J., Petersen, R.C., Snyder, P.J., Carrillo, M.C., Thies, B., Phelps, C.H., 2011. The diagnosis of mild cognitive impairment due to Alzheimer's disease: Recommendations from the National Institute on Aging-Alzheimer's Association workgroups on diagnostic guidelines for Alzheimer's disease. Alzheimer's Dement. 7, 270–279. https://doi.org/10.1016/j.jalz.2011.03.008.

Arriagada, P.V., Growdon, J.H., Hedley-Whyte, E.T., Hyman, B.T., 1992. Neurofibrillary tangles but not senile plaques parallel duration and severity of Alzheimer's disease. Neurology 42, 631–639. https://doi.org/10.1212/WNL.42.3.631.

Bang, J., Spina, S., Miller, B.L., 2015. Frontotemporal dementia. Lancet 386, 1672–1682. https://doi.org/10.1016/S0140-6736(15)00461-4.

Buciuc, M., Duffy, J.R., Machulda, M.M., Graff-Radford, J., Thu Pham, N.T., Martin, P.R., Senjem, M.L., Jack, C.R., Ertekin-Taner, N., Dickson, D.W., Lowe, V.J., Whitwell, J. L., Josephs, K.A., 2021. Clinical, Imaging, and Pathologic Characteristics of Patients With Right Versus Left Hemisphere-Predominant Logopenic Progressive Aphasia. Neurology 97, e523–e534. https://doi.org/10.1212/wnl.0000000000012322.

Chhatwal, J.P., Schultz, S.A., McDade, E., Schultz, A.P., Liu, L., Hanseeuw, B.J., Joseph-Mathurin, N., Feldman, R., Fitzpatrick, C.D., Sparks, K.P., Levin, J., Berman, S.B., Renton, A.E., Esposito, B.T., Fernandez, M.V., Sung, Y.J., Lee, J.H., Klunk, W.E., Hofmann, A., Noble, J.M., Graff-Radford, N., Mori, H., Salloway, S.M., Masters, C.L., Martins, R., Karch, C.M., Xiong, C., Cruchaga, C., Perrin, R.J., Gordon, B.A., Benzinger, T.L.S., Fox, N.C., Schofield, P.R., Fagan, A.M., Goate, A.M., Morris, J.C., Bateman, R.J., Johnson, K.A., Sperling, R.A., 2022. Variant-dependent heterogeneity in amyloid β burden in autosomal dominant Alzheimer's disease: cross-sectional and longitudinal analyses of an observational study. Lancet Neurol. 21, 140–152. https://doi.org/10.1016/S1474-4422(21)00375-6.

Cho, H., Choi, J.Y., Lee, S.H., Lee, J.H., Choi, Y.C., Ryu, Y.H., Lee, M.S., Lyoo, C.H., 2017. Excessive tau accumulation in the parieto-occipital cortex characterizes early-onset Alzheimer's disease. Neurobiol. Aging 53, 103–111. https://doi.org/10.1016/j.neurobiolaging.2017.01.024.

Chong, J.R., Ashton, N.J., Karikari, T.K., Tanaka, T., Saridin, F.N., Reilhac, A., Robins, E. G., Nai, Y.H., Vrooman, H., Hilal, S., Zetterberg, H., Blennow, K., Lai, M.K.P., Chen, C.P., 2021. Plasma P-tau181 to Aβ42 ratio is associated with brain amyloid burden and hippocampal atrophy in an Asian cohort of Alzheimer's disease patients with concomitant cerebrovascular disease. Alzheimer's Dement. 17, 1649–1662. https://doi.org/10.1002/alz.12332.

Collij, L.E., Salvadó, G., Wottschel, V., Mastenbroek, S.E., Schoenmakers, P., Heeman, F., Aksman, L., Wink, A.M., Berckel, B.N.M., van de Flier, W.M., Scheltens, P., Visser, P. J., Barkhof, F., Haller, S., Gispert, J.D., Lopes Alves, I., 2022. Spatial-Temporal Patterns of β-Amyloid Accumulation: A Subtype and Stage Inference Model Analysis. Neurology 98 (17), e1692–e1703.

Di Stasio, F., Suppa, A., Marsili, L., Upadhyay, N., Asci, F., Bologna, M., Colosimo, C., Fabbrini, G., Pantano, P., Berardelli, A., 2019. Corticobasal syndrome: neuroimaging and neurophysiological advances. Eur. J. Neurol. 26, 50–52. https://doi.org/10.1111/ene.13928.

Duboc, V., Dufourcq, P., Blader, P., Roussigné, M., 2015. Asymmetry of the Brain: Development and Implications. Annu. Rev. Genet. 49, 647–672. https://doi.org/10.1146/annurev-genet-112414-055322.

Dubois, B., Feldman, H.H., Jacova, C., Hampel, H., Molinuevo, J.L., Blennow, K., Dekosky, S.T., Gauthier, S., Selkoe, D., Bateman, R., Cappa, S., Crutch, S., Engelborghs, S., Frisoni, G.B., Fox, N.C., Galasko, D., Habert, M.O., Jicha, G.A., Nordberg, A., Pasquier, F., Rabinovici, G., Robert, P., Rowe, C., Salloway, S., Sarazin, M., Epelbaum, S., de Souza, L.C., Vellas, B., Visser, P.J., Schneider, L., Stern, Y., Scheltens, P., Cummings, J.L., 2014. Advancing research diagnostic criteria for Alzheimer's disease: The IWG-2 criteria. Lancet Neurol. 13, 614–629. https://doi.org/10.1016/S1474-4422(14)70090-0.

Dujardin, S., Commins, C., Lathuiliere, A., Beerepoot, P., Fernandes, A.R., Kamath, T.V., De Los Santos, M.B., Klickstein, N., Corjuc, D.L., Corjuc, B.T., Dooley, P.M., Viode, A., Oakley, D.H., Moore, B.D., Mullin, K., Jean-Gilles, D., Clark, R., Atchison, K., Moore, R., Chibnik, L.B., Tanzi, R.E., Frosch, M.P., Serrano-Pozo, A., Elwood, F., Steen, J.A., Kennedy, M.E., Hyman, B.T., 2020. Tau molecular diversity contributes to clinical heterogeneity in Alzheimer's disease. Nat. Med. 26, 1256–1263. https://doi.org/10.1038/s41591-020-0938-9.

Fjell, A.M., Grydeland, H., Krogsrud, S.K., Amlien, I., Rohani, D.A., Ferschmann, L., Storsve, A.B., Tamnes, C.K., Sala-Llonch, R., Due-Tønnessen, P., Bjørnerud, A., Sølsnes, A.E., Håberg, A.K., Skranes, J., Bartsch, H., Chen, C.H., Thompson, W.K., Panizzon, M.S., Kremen, W.S., Dale, A.M., Walhovd, K.B., 2015. Development and aging of cortical thickness correspond to genetic organization patterns. Proc. Natl. Acad. Sci. U. S. A. 112, 15462–15467. https://doi.org/10.1073/pnas.1508831112.

Frings, L., Hellwig, S., Spehl, T.S., Bormann, T., Buchert, R., Vach, W., Minkova, L., Heimbach, B., Klöppel, S., Meyer, P.T., 2015. Asymmetries of amyloid-β burden and neuronal dysfunction are positively correlated in Alzheimer's disease. Brain 138, 3089–3099. https://doi.org/10.1093/brain/awv229.

Gefen, T., Gasho, K., Rademaker, A., Lalehzari, M., Weintraub, S., Rogalski, E., Wieneke, C., Bigio, E., Geula, C., Mesulam, M.M., 2012. Clinically concordant variations of Alzheimer pathology in aphasic versus amnestic dementia. Brain 135, 1554–1565. https://doi.org/10.1093/brain/aws076.

Goedert, M., 2015. Alzheimer's and Parkinson's diseases: The prion concept in relation to assembled Aβ, tau, and α-synuclein. Science (80-.) 349, 61–69. https://doi.org/10.1126/science.1255555.

Jack, C.R., Bennett, D.A., Blennow, K., Carrillo, M.C., Dunn, B., Haeberlein, S.B., Holtzman, D.M., Jagust, W., Jessen, F., Karlawish, J., Liu, E., Molinuevo, J.L., Montine, T., Phelps, C., Rankin, K.P., Rowe, C.C., Scheltens, P., Siemers, E., Snyder, H.M., Sperling, R., Elliott, C., Masliah, E., Ryan, L., Silverberg, N., 2018. NIA-AA Research Framework: Toward a biological definition of Alzheimer's disease. Alzheimer's Dement. 14 (4), 535–562.

Jack, C.R., Wiste, H.J., Weigand, S.D., Therneau, T.M., Lowe, V.J., Knopman, D.S., Botha, H., Graff-Radford, J., Jones, D.T., Ferman, T.J., Boeve, B.F., Kantarci, K., Vemuri, P., Mielke, M.M., Whitwell, J., Josephs, K., Schwarz, C.G., Senjem, M.L., Gunter, J.L., Petersen, R.C., 2020. Predicting future rates of tau accumulation on PET. Brain 143, 3136–3150. https://doi.org/10.1093/brain/awaa248.

Jagust, W., 2018. Imaging the evolution and pathophysiology of Alzheimer disease. Nat. Rev. Neurosci. 19, 687–700. https://doi.org/10.1038/s41583-018-0067-3.

Joie, R.L., Visani, A.V., Baker, S.L., Brown, J.A., Bourakova, V., Cha, J., Chaudhary, K., Edwards, L., Iaccarino, L., Janabi, M., Lesman-Segev, O.H., Miller, Z.A., Perry, D.C., O'Neil, J.P., Pham, J., Rojas, J.C., Rosen, H.J., Seeley, W.W., Tsai, R.M., Miller, B.L., Jagust, W.J., Rabinovici, G.D., 2020. Prospective longitudinal atrophy in Alzheimer's disease correlates with the intensity and topography of baseline tau-PET. Sci. Transl. Med. 12, eaau5732. https://doi.org/10.1126/scitranslmed.aau5732.

Knopman, D.S., Amieva, H., Petersen, R.C., Chételat, G., Holtzman, D.M., Hyman, B.T., Nixon, R.A., Jones, D.T., 2021. Alzheimer disease. Nat. Rev. Dis. Prim. 7, 33. https://doi.org/10.1038/s41572-021-00269-y.

S. Landau W. Jagust ADNI Florbetapir processing methods [WWW Document] 2015 https://adni.bitbucket.io/reference/docs/UCBERKELEYAV45/ADNI_AV45_Methods_JagustLab_06.25.15.pdf.

Lehmann, M., Ghosh, P.M., Madison, C., Laforce, R., Corbetta-Rastelli, C., Weiner, M.W., Greicius, M.D., Seeley, W.W., Gorno-Tempini, M.L., Rosen, H.J., Miller, B.L., Jagust, W.J., Rabinovici, G.D., 2013. Diverging patterns of amyloid deposition and hypometabolism in clinical variants of probable Alzheimer's disease. Brain 136 (3), 844–858.

Li, P., Ensink, E., Lang, S., Marshall, L., Schilthuis, M., Lamp, J., Vega, I., Labrie, V., 2020. Hemispheric asymmetry in the human brain and in Parkinson's disease is linked to divergent epigenetic patterns in neurons. Genome Biol. 21, 61. https://doi.org/10.1186/s13059-020-01960-1.

Li, G., Lin, W., Gilmore, J.H., Shen, D., 2015. Spatial Patterns, Longitudinal Development, and Hemispheric Asymmetries of Cortical Thickness in Infants from Birth to 2 Years of Age. J. Neurosci. 35, 9150–9162. https://doi.org/10.1523/JNEUROSCI.4107-14.2015.

Li, L., Liu, F.T., Li, M., Lu, J.Y., Sun, Y.M., Liang, X., Bao, W., Chen, Q.S., Li, X.Y., Zhou, X.Y., Guan, Y., Wu, J.J., Yen, T.C., Jang, M.K., Luo, J.F., Wang, J., Zuo, C., 2021. Clinical Utility of 18F-APN-1607 Tau PET Imaging in Patients with Progressive Supranuclear Palsy. Mov. Disord. 36, 2314–2323. https://doi.org/10.1002/mds.28672.

Lundeen, T.F., Seibyl, J.P., Covington, M.F., Eshghi, N., Kuo, P.H., 2018. Signs and artifacts in amyloid PET. Radiographics 38, 2123–2133. https://doi.org/10.1148/rg.2018180160.

Marquié, M., Normandin, M.D., Vanderburg, C.R., Costantino, I.M., Bien, E.A., Rycyna, L. G., Klunk, W.E., Mathis, C.A., Ikonomovic, M.D., Debnath, M.L., Vasdev, N., Dickerson, B.C., Gomperts, S.N., Growdon, J.H., Johnson, K.A., Frosch, M.P., Hyman, B.T., Gómez-Isla, T., 2015. Validating novel tau positron emission tomography tracer [F-18]-AV-1451 (T807) on postmortem brain tissue. Ann. Neurol. 78, 787–800. https://doi.org/10.1002/ana.24517.

Marquié, M., Normandin, M.D., Meltzer, A.C., Siao Tick Chong, M., Andrea, N.V., Antón-Fernández, A., Klunk, W.E., Mathis, C.A., Ikonomovic, M.D., Debnath, M., Bien, E.A., Vanderburg, C.R., Costantino, I., Makaretz, S., DeVos, S.L., Oakley, D.H., Gomperts, S.N., Growdon, J.H., Domoto-Reilly, K., Lucente, D., Dickerson, B.C., Frosch, M.P., Hyman, B.T., Johnson, K.A., Gómez-Isla, T., 2017. Pathological correlations of [F-18]-AV-1451 imaging in non-alzheimer tauopathies. Ann. Neurol. 81 (1), 117–128.

Marshall, G.A., Fairbanks, L.A., Tekin, S., Vinters, H.V., Cummings, J.L., 2007. Early-Onset Alzheimer's Disease Is Associated With Greater Pathologic Burden. J. Geriatr. Psychiatry Neurol. 20, 29–33. https://doi.org/10.1177/0891988706297086.

Mc Auley, M.T., 2021. DNA Methylation in Genes Associated with the Evolution of Ageing and Disease: A Critical Review. Ageing Res. Rev. 72, 101488 https://doi.org/10.1016/j.arr.2021.101488.

McKhann, G.M., Knopman, D.S., Chertkow, H., Hyman, B.T., Jack, C.R., Kawas, C.H., Klunk, W.E., Koroshetz, W.J., Manly, J.J., Mayeux, R., Mohs, R.C., Morris, J.C., Rossor, M.N., Scheltens, P., Carrillo, M.C., Thies, B., Weintraub, S., Phelps, C.H., 2011. The diagnosis of dementia due to Alzheimer's disease: Recommendations from the National Institute on Aging-Alzheimer's Association workgroups on diagnostic guidelines for Alzheimer's disease. Alzheimer's Dement. 7 (3), 263–269.

Murray, M.E., Graff-Radford, N.R., Ross, O.A., Petersen, R.C., Duara, R., Dickson, D.W., 2011. Neuropathologically defined subtypes of Alzheimer's disease with distinct

clinical characteristics: A retrospective study. Lancet Neurol. 10, 785–796. https://doi.org/10.1016/S1474-4422(11)70156-9.

Nasrallah, I.M., Chen, Y.J., Hsieh, M.K., Phillips, J.S., Ternes, K., Stockbower, G.E., Sheline, Y., McMillan, C.T., Grossman, M., Wolk, D.A., 2018. 18F-flortaucipir PET/MRI correlations in nonamnestic and amnestic variants of Alzheimer disease. J. Nucl. Med. 59, 299–306. https://doi.org/10.2967/jnumed.117.194282.

Ohm, D.T., Fought, A.J., Rademaker, A., Kim, G., Sridhar, J., Coventry, C., Gefen, T., Weintraub, S., Bigio, E., Mesulam, M.M., Rogalski, E., Geula, C., 2020. Neuropathologic basis of in vivo cortical atrophy in the aphasic variant of Alzheimer's disease. Brain Pathol. 30, 332–344. https://doi.org/10.1111/bpa.12783.

Ossenkoppele, R., Schonhaut, D.R., Schöll, M., Lockhart, S.N., Ayakta, N., Baker, S.L., O'Neil, J.P., Janabi, M., Lazaris, A., Cantwell, A., Vogel, J., Santos, M., Miller, Z.A., Bettcher, B.M., Vossel, K.A., Kramer, J.H., Gorno-Tempini, M.L., Miller, B.L., Jagust, W.J., Rabinovici, G.D., 2016. Tau PET patterns mirror clinical and neuroanatomical variability in Alzheimer's disease. Brain 139, 1551–1567. https://doi.org/10.1093/brain/aww027.

Postema, M.C., van Rooij, D., Anagnostou, E., Arango, C., Auzias, G., Behrmann, M., Filho, G.B., Calderoni, S., Calvo, R., Daly, E., Deruelle, C., Di Martino, A., Dinstein, I., Duran, F.L.S., Durston, S., Ecker, C., Ehrlich, S., Fair, D., Fedor, J., Feng, X., Fitzgerald, J., Floris, D.L., Freitag, C.M., Gallagher, L., Glahn, D.C., Gori, I., Haar, S., Hoekstra, L., Jahanshad, N., Jalbrzikowski, M., Janssen, J., King, J.A., Kong, X.Z., Lazaro, L., Lerch, J.P., Luna, B., Martinho, M.M., McGrath, J., Medland, S.E., Muratori, F., Murphy, C.M., Murphy, D.G.M., O'Hearn, K., Oranje, B., Parellada, M., Puig, O., Retico, A., Rosa, P., Rubia, K., Shook, D., Taylor, M.J., Tosetti, M., Wallace, G.L., Zhou, F., Thompson, P.M., Fisher, S.E., Buitelaar, J.K., Francks, C., 2019. Altered structural brain asymmetry in autism spectrum disorder in a study of 54 datasets. Nat. Commun. 10, 4958. https://doi.org/10.1038/s41467-019-13005-8.

Roe, J.M., Vidal-Piñeiro, D., Sørensen, Ø., Brandmaier, A.M., Düzel, S., Gonzalez, H.A., Kievit, R.A., Knights, E., Kühn, S., Lindenberger, U., Mowinckel, A.M., Nyberg, L., Park, D.C., Pudas, S., Rundle, M.M., Walhovd, K.B., Fjell, A.M., Westerhausen, R., Masters, C.L., Bush, A.I., Fowler, C., Darby, D., Pertile, K., Restrepo, C., Roberts, B., Robertson, J., Rumble, R., Ryan, T., Collins, S., Thai, C., Trounson, B., Lennon, K., Li, Q.X., Ugarte, F.Y., Volitakis, I., Vovos, M., Williams, R., Baker, J., Russell, A., Peretti, M., Milicic, L., Lim, L., Rodrigues, M., Taddei, K., Taddei, T., Hone, E., Lim, F., Fernandez, S., Rainey-Smith, S., Pedrini, S., Martins, R., Doecke, J., Bourgeat, P., Fripp, J., Gibson, S., Leroux, H., Hanson, D., Dore, V., Zhang, P., Burnham, S., Rowe, C.C., Villemagne, V.L., Yates, P., Pejoska, S.B., Jones, G., Ames, D., Cyarto, E., Lautenschlager, N., Barnham, K., Cheng, L., Hill, A., Killeen, N., Maruff, P., Silbert, B., Brown, B., Sohrabi, H., Savage, G., Vacher, M., 2021. Asymmetric thinning of the cerebral cortex across the adult lifespan is accelerated in Alzheimer's disease. Nat. Commun. 12, 721. https://doi.org/10.1038/s41467-021-21057-y.

Rolls, E.T., Huang, C.C., Lin, C.P., Feng, J., Joliot, M., 2020. Automated anatomical labelling atlas 3. Neuroimage 206, 116189. https://doi.org/10.1016/j.neuroimage.2019.116189.

Samii, A., Nutt, J.G., Ransom, B.R., 2004. Parkinson's disease. Lancet 363, 1783–1793. https://doi.org/10.1016/S0140-6736(04)16305-8.

Schmidt, C., Wolff, M., Weitz, M., Bartlau, T., Korth, C., Zerr, I., Review, N., 2011. Rapidly Progressive Alzheimer Disease. Arch. Neurol. 68, 1124–1130. https://doi.org/10.1001/archneurol.2011.189.

Shi, Z., Fu, L., Zhang, N., Zhao, X., Liu, S., Zuo, C., Cai, L., Wang, Y., Gao, S., Ai, L., Guan, Y.H., Xu, B., Ji, Y., 2020. Amyloid PET in Dementia Syndromes: A Chinese Multicenter Study. J. Nucl. Med. 61, 1814–1819. https://doi.org/10.2967/jnumed.119.240325.

Smirnov, D.S., Galasko, D., Hiniker, A., Edland, S.D., Salmon, D.P., 2021. Age-at-Onset and APOE-Related Heterogeneity in Pathologically Confirmed Sporadic Alzheimer Disease. Neurology 96, e2272–e2283. https://doi.org/10.1212/WNL.0000000000011772.

Smirnov, D.S., Ashton, N.J., Blennow, K., Zetterberg, H., Simrén, J., Lantero-Rodriguez, J., Karikari, T.K., Hiniker, A., Rissman, R.A., Salmon, D.P., Galasko, D., 2022. Plasma biomarkers for Alzheimer's Disease in relation to neuropathology and cognitive change. Acta Neuropathol. 143, 487–503. https://doi.org/10.1007/s00401-022-02408-5.

Soto, M.E., Andrieu, S., Arbus, C., Ceccaldi, M., Couratier, P., Dantoine, T., Dartigues, J.-F., Gillette-Guyonette, S., Nourhashemi, F., Ousset, P.-J., 2008. Rapid cognitive decline in Alzheimer's disease. Consensus paper. J. Nutr. Health Aging 12, 703–713. https://doi.org/10.1007/BF03028618.

Tagai, K., Ono, M., Kubota, M., Kitamura, S., Takahata, K., Seki, C., Takado, Y., Shinotoh, H., Sano, Y., Yamamoto, Y., Matsuoka, K., Takuwa, H., Shimojo, M., Takahashi, M., Kawamura, K., Kikuchi, T., Okada, M., Akiyama, H., Suzuki, H., Onaya, M., Takeda, T., Arai, K., Arai, N., Araki, N., Saito, Y., Trojanowski, J.Q., Lee, V.M.Y., Mishra, S.K., Yamaguchi, Y., Kimura, Y., Ichise, M., Tomita, Y., Zhang, M.R., Suhara, T., Shigeta, M., Sahara, N., Higuchi, M., Shimada, H., 2021. High-Contrast In Vivo Imaging of Tau Pathologies in Alzheimer's and Non-Alzheimer's Disease Tauopathies. Neuron 109, 42–58.e8. https://doi.org/10.1016/j.neuron.2020.09.042.

Tetzloff, K.A., Graff-Radford, J., Martin, P.R., Tosakulwong, N., Machulda, M.M., Duffy, J.R., Clark, H.M., Senjem, M.L., Schwarz, C.G., Spychalla, A.J., Drubach, D.A., Jack, C.R., Lowe, V.J., Josephs, K.A., Whitwell, J.L., 2018. Regional Distribution, Asymmetry, and Clinical Correlates of Tau Uptake on [18F]AV-1451 PET in Atypical Alzheimer's Disease. J. Alzheimer's Dis. 62, 1713–1724. https://doi.org/10.3233/JAD-170740.

Vogel, J.W., Young, A.L., Oxtoby, N.P., Smith, R., Ossenkoppele, R., Strandberg, O.T., La Joie, R., Aksman, L.M., Grothe, M.J., Iturria-Medina, Y., Pontecorvo, M.J., Devous, M.D., Rabinovici, G.D., Alexander, D.C., Lyoo, C.H., Evans, A.C., Hansson, O., 2021. Four distinct trajectories of tau deposition identified in Alzheimer's disease. Nat. Med. 27 (5), 871–881.

Wang, D., Buckner, R.L., Liu, H., 2014. Functional Specialization in the Human Brain Estimated By Intrinsic Hemispheric Interaction. J. Neurosci. 34, 12341–12352. https://doi.org/10.1523/JNEUROSCI.0787-14.2014.

Weise, C.M., Chen, K., Chen, Y., Kuang, X., Savage, C.R., Reiman, E.M., 2018. Left lateralized cerebral glucose metabolism declines in amyloid-β positive persons with mild cognitive impairment. NeuroImage Clin. 20, 286–296. https://doi.org/10.1016/j.nicl.2018.07.016.

Xiao, Z., Wu, X., Wu, W., Yi, J., Liang, X., Ding, S., Zheng, L., Luo, J., Gu, H., Zhao, Q., Xu, H., Ding, D., 2021. Plasma biomarker profiles and the correlation with cognitive function across the clinical spectrum of Alzheimer's disease. Alzheimers. Res. Ther. 13, 123. https://doi.org/10.1186/s13195-021-00864-x.

Yoon, H.J., Kim, B.S., Jeong, J.H., Kim, G.H., Park, H.K., Chun, M.Y., 2021. Asymmetric Amyloid Deposition as an Early Sign of Progression in Mild Cognitive Impairment Due to Alzheimer Disease. Clin. Nucl. Med. 46, 527–531. https://doi.org/10.1097/RLU.0000000000003662.

Young, C.B., Winer, J.R., Younes, K., Cody, K.A., Betthauser, T.J., Johnson, S.C., Schultz, A., Sperling, R.A., Greicius, M.D., Cobos, I., Poston, K.L., Mormino, E.C., Weiner, M.W., Aisen, P., Petersen, R., Jack, C.R., Jagust, W., Trojanowki, J.Q., Toga, A.W., Beckett, L., Green, R.C., Saykin, A.J., Morris, J.C., Perrin, R.J., Shaw, L.M., Khachaturian, Z., Carrillo, M., Potter, W., Barnes, L., Bernard, M., Gonzalez, H., Ho, C., Hsiao, J.K., Jackson, J., Masliah, E., Masterman, D., Okonkwo, O., Ryan, L., Silverberg, N., Fleisher, A., Sacrey, D.T., Fockler, J., Conti, C., Veitch, D., Neuhaus, J., Jin, C., Nosheny, R., Ashford, M., Flenniken, D., Kormos, A., Montine, T., Rafii, M., Raman, R., Jimenez, G., Donohue, M., Gessert, D., Salazar, J., Zimmerman, C., Cabrera, Y., Walter, S., Miller, G., Coker, G., Clanton, T., Hergesheimer, L., Smith, S., Adegoke, O., Mahboubi, P., Moore, S., Pizzola, J., Shaffer, E., Harvey, D., Forghanian-Arani, A., Borowski, B., Ward, C., Schwarz, C., Jones, D., Gunter, J., Kantarci, K., Senjem, M., Vemuri, P., Reid, R., Fox, N.C., Malone, I., Thompson, P., Thomopoulos, S.I., Nir, T.M., Jahanshad, N., DeCarli, C., Knaack, A., Fletcher, E., Tosun-Turgut, D., Chen, S.R., Choe, M., Crawford, K., Yuschkevich, P.A., Das, S., Koeppe, R.A., Reiman, E.M., Chen, K., Mathis, C., Landau, S., Cairns, N.J., Householder, E., Franklin, E., Bernhardt, H., Taylor-Reinwald, L., Korecka, M., Figurski, M., Neu, S., Nho, K., Risacher, S.L., Apostolova, L.G., Shen, L.i., Foroud, T.M., Nudelman, K., Faber, K., Wilmes, K., Thal, L., Johnson, K.A., Sperling, R.A., 2022. Divergent Cortical Tau Positron Emission Tomography Patterns among Patients with Preclinical Alzheimer Disease. JAMA Neurol. 79 (6), 592.

Ziffra, R.S., Kim, C.N., Ross, J.M., Wilfert, A., Turner, T.N., Haeussler, M., Casella, A.M., Przytycki, P.F., Keough, K.C., Shin, D., Bogdanoff, D., Kreimer, A., Pollard, K.S., Ament, S.A., Eichler, E.E., Ahituv, N., Nowakowski, T.J., 2021. Single-cell epigenomics reveals mechanisms of human cortical development. Nature 598 (7879), 205–213.